International Journal of Urology and Nephrology ISSN 2091-1254 Vol. 4 (1), pp. 101-109, January, 2016. Available online at www.internationalscholarsjournals.org © International Scholars Journals

Full Length Research Paper

Analysis of proteomic and acute kidney allograft rejection in rat

Wu Yi[1], Li Peng[2] and Wang Xueqian[3]

[1]Department of Urology, the First Affiliated Hospital, Chongqing Medical University, Chongqing, 400016, China.
[2]Department of Emergency, the First Affiliated Hospital, Chongqing Medical University, Chongqing, 400016, China.
[3]Department of Laboratory Medicine, the First Affiliated Hospital, Chongqing Medical University, Chongqing, 400016, China. *Corresponding author. E-mail: wu_yi2012@gmail.com.

Received 12 October, 2015; Revised 04 January, 2016; Accepted 10 January 2016 and Published 22 January, 2016

Kidney transplantation to treat end-stage renal disease has evolved rapidly from the first successful transplantations to the current widespread use of grafts from both cadaveric and living donors. But acute rejection is still a strong risk factor for chronic rejection in recipients of renal grafts. To investigate possible mechanisms, we describe a comparison between different proteins expression profile of acute rejection and the controls. Through two-dimensional difference gel electrophoresis, mass spectral techniques microarray analysis and quantitative real-time RT-PCR confirmation, marked change in expression level of 37 protein spots was observed in allograft rejection group. Among them, expression levels of 24 protein spots were up-regulated, while expression levels of 13 protein spots were down-regulated. Among 37 protein spots, 29 obtained satisfactory peptide mass fingerprinting. We identified 6 proteins in acute rejection after renal transplantation. Then, we investigated PDIA3 levels in serum and transplanted kidney, PDIA3 mRNA and protein expression level. Our data thus indicate that PDIA3 might be potentially involved into the occurrence and development of acute rejection response in renal transplantation.

Key words: PDIA3, mass spectrum, acute rejection, renal transplantation.

INTRODUCTION

Renal transplantation is the preferred treatment method of endstage renal disease (ESRD). It is more cost-effective than is maintenance dialysis (United Network for Organ Sharing, 1994) and usually provides the patient with a better quality of life (Wong, 2011). Despite several advances in the field of transplantation, renal transplant recipients continue to be at high risk of developing various infectious and non-infectious complications. Adjusted mortality risk ratios indicate a significant reduction in mortality for kidney transplantation recipients when compared with that for patients receiving dialysis and patients receiving dialysis who are on a waiting list for renal transplantation.

The indication for renal transplantation is irreversible renal failure that requires or will soon require long-term dialytic therapy. Proteomic analysis could have a wide application in the field of organ transplantation by providing unique information about cells and tissues in transplanted patients and eventually creating non-invasive tests to monitor biomarkers in body fluids, such as urine or blood, that would correlate with transplant rejection, function and immunosuppression. A proteomics application to monitor transplantation acceptance was reported by Pan et al. (2004) using 2D PAGE and MALDI-TOF in a rat model of liver transplantation. Mass spectral techniques, although criticized for sensitivity

issues (especially compared to ELISA and RT-PCR) (Diamandis, 2004) have the strong advantage that they are useful in the analysis of components of a mixture without prior identification. In the present study, we analyse the difference of proteins expression in rat isograft group and allograft group, using two-dimensional difference gel electrophoresis and mass spectral techniques. This study help us to find protein markers related to acute rejection in renal transplantation. We still explore relationship between differentially expressed proteins and acute rejection in renal transplantation.

MATERIALS AND METHODS

Animals

Male 8 to 10-week-old Lewis and F344 inbred male rats (180 to 200 g) purchased from the University Animal Breeding and Research Center (Changqin, China) were housed and cared for using protocols approved by our Subcommittee on Research Animal Care. The rats were divided into 4 groups: an allogeneic (experiment) group (n=8 pair) of Lewis recipients receiving F344 renal grafts; a syngeneic (control) group (n=8 pair), of F344 recipients receiving F344 renal grafts.

Rat renal transplantation

Orthotopic kidney transplantation was performed using a previously described technique (Neto et al., 2006; Nakao et al., 2009). In short, after intravenous heparinization (300 U), the donor's left kidney was removed with the left renal artery in continuity with a short aortic segment and the left renal vein with a patch of venacava. The excised graft was flushed with 3 ml of UW solution (Viaspan, Du Pont, Wilmington, DE). The left kidney graft was orthotopically transplanted into the recipient by end-to-side microvascular anastomoses between graft aorta and recipient infrarenal abdominal aorta, and between graft renal vein and recipient infrarenal vena cava with 10 to 0 Micrin suture. Both native kidneys of the recipient were removed, and end-to-end ureteral anastomosis was performed using 10 to 0 Micrin suture. Recipients received prophylactic antibiotics (Cefotetan disodium, 100 mg/kg, intramuscular injection) for 3 days following the transplantation.

Animals were sacrificed 1 week after the renal transplant procedure and kidney was recovered for histological analysis. The kidneys were fixed in a 10% neutral buffered formalin solution, embedded in paraffin and used for histopathological examination. Four micrometer thick sections were cut, desparaffinized hydrated and stained with hematoxylin and eosin. The renal sections were examined on a blind fashion for the grade of cortical tubular epithelial necrosis. Counts were performed in at least 10 different fields of square micrometers and assigned for the severity of necrosis, using scores on a scale of 1 (< 5%), 2 (6 to 25%), 3 (26 to 50%), 4 (51 to 75%) and 5 (>75%). Blood creatinine determination was performed. Values are expressed as the difference between pre-transplant and post-trasplant for each group. The excised kidney grafts were split with some parts immersed in 10% formalin for histology, and others stored in liquid nitrogen for reverse transcriptase–polymerase chain reaction (RT-PCR).

2-DE

Pooled 50 µl fractions were mixed with 85 µl rehydration buffer, containing 8 M urea, 2% (w/v) CHAPS, 50 mM DTT, 1 mM PMSF and carrier ampholytes. The following operations for all samples were processed under the same conditions. Focusing was carried out in 7 cm strip (Amersham Biosciences) with a pH range of 3 to 10 (NL) at 20°C covered with mineral oil. IEF was performed on an IPGphor (Amersham Biosciences). Rehydration of the IPG strip with sample was carried out for 12 h at low voltage (6 h at 30 V and 6 h at 50 V). The electrophoretic conditions during IEF were as following: 1 h at 250 V, 1 h at 500 V, 1 h at 1000 V, 1 h at 2000 V, 6 h at 4000 V and 12 h at 500 V. As soon as electrophoresis was completed, the strips were drained of excess oil and used immediately, or stored at −20°C for subsequent loading onto the second dimension.

After IEF, the strips were equilibrated for 15 min twice, by gentle shaking in 2 ml solution containing Tris–HCl buffer (50 mM, pH 6.8), 6 M urea, 30% (v/v) glycerol and 2% (w/v) SDS. DTT (2%, w/v) was added to the first to keep sulfhydryl groups reduced, and 2.5% (w/v) iodoacetamide was added to the second to alkylate sulfhydryl. Strips were then embedded on top of 12% SDS-PAGE gel using 0.5% (w/v) agarose in the electrophoresis buffer colored with a trace of bromophenol blue. Second dimensional electrophoresis was performed at 10°C using 20 mA/gel until the dye front reached the bottom of the SDS-PAGE gel using a Protean IIxi system (Bio-Rad). Gels were stained with Coomassie brilliant blue staining. The stained gels were scanned using an ImageScanner (Amersham Pharmacia) and analyzed with ImageMaster software (Amersham Pharmacia).

In-gel trypsin digestion of proteins

Protein spots of interest were cut manually from the gel and diced into small pieces (<1 mm) with a stainless steel scalpel and placed into siliconized microcentrifuge tubes. The gel fragments were de-stained and dehydrated by washing two times for 10 to 15 min with 25 mM NH_4HCO_3 in 50% acetonitrile until shrunken and white. For heavily stained spots that were not completely de-stained after a third wash, 100 µl of water was added to rehydrate the gel followed by an additional treatment with 25 mM NH_4HCO_3 in 50% acetonitrile. The de-stained gel particles were then dried for 30 min under vacuum in a Speed-Vac vacuum concentrator (Savant, Holbrook, NY). 40 µl of a trypsin solution (0.025 mg ml^{-1}) were added to each tube. Rehydration of the gel pieces was complete over 15 min at 4°C to minimize trypsin auto-proteolysis. (If necessary, 25 mM NH_4HCO_3 solution was added until gel pieces were fully covered with liquid).

Tubes were sealed with parafilm and digestion was performed for 16 h at 37°C in a water bath. When digestion was complete, 100 µl of water was added and tubes were sonicated for 10 min. The supernatant was removed from each tube and transferred into a fresh tube. Further recovery of the peptides was accomplished by extracting twice with 50% acetonitrile/5% trifluoroacetic acid. All supernatants were pooled and placed in a Speed-Vac concentrator to minimize volatile salts by reducing the volume to ~5 µl. Extracts were taken up in 100 µl of water and dried down again three times until no salt residue was visible at the tube walls. After the last drying step, 15 µl of 50% acetonitrile/5% trifluoroacetic acid was added. Control digests were performed on gel slices that did not contain any protein and were typically found at the sides of the gel. Trypsin autoproteolysis products and CCB dye contaminants could be identified in the subsequent mass spectrometric analyses and manually subtracted.

Mass spectrometry

As described in Keeping et al. (2011), a small fraction (0.5 µl) of the unseparated tryptic digest mixture was mixed with α-cyano-4-hydroxycinnamic acid matrix (1:1, v/v) and analyzed on an Applied

Biosystems Voyager DeSTR matrix-assisted laser desorption ionization time-of-flight (MALDI-TOF) mass spectrometer with a nitrogen laser, operated in delayed extraction (Vestal et al., 1995) and reflectron mode. A standard peptide mixture consisting of angiotensin, bradykinin, bombesin, and adrenocorticotropic hormone fragment 18 to 39 was used to provide an external mass calibration. Post-source decay (PSD) analysis of peptides involved timed ion selection of the corresponding precursor molecular ion (MH+) followed by focusing of the product metastable fragment ions.

The PSD experiments were carried out by sequential focusing of mass segments by varying the reflectron voltage in 12 steps. The complete spectrum was reassembled by stitching the individual mass segments together. Calibration in PSD mode was carried out by a one-point correction of the parent ion obtained in the first mass segment. Both the relative molecular weight (Mr) and the isoelectric point (pI) of the intact protein, as judged from the 2-DGs, were used as further criteria for protein identification. For most of the identified proteins, two to four tryptic peptides were matched by mass and sequence to the top candidates retrieved by the searches. No second-pass searches were performed to identify any less abundant proteins that might co-migrate with the major proteins. To classify identified proteins, functional information was retrieved mainly from the Swiss-Prot database (http://us.expasy.org/sprot/).

Immunohistochemical staining

Immunohistochemical staining of the 8 µm frozen sections were performed with the Strept–Avidin–Biotin–Peroxidase complex (SABC) method, using a SABC Kit (Boster Co, Wuhan, China). Briefly 8 µm sections were treated with 0.3% hydrogen peroxide and incubated with 10% normal goat serum to block non-specific binding. The sections were then incubated with rabbit anti-human PDIA3 monoclonal antibody (diluted 1:100, Santa Cruz Biotechnology, Santa Cruz, CA, USA) or control rabbit serum at room temperature for 2 h, and were washed in 0.01 M PBS and exposed to biotinylated goat anti-rabbit IgG, followed by treatment with the Strept–Avidin–Biotin–Peroxidase complex and stained with diaminobenzidine with 0.15% hydrogen peroxide. PBS takes the place of PDIA3 antibody as the negative staining control.

Counterstaining was performed with haematoxylin. The intensity of immunostaining was assessed by two independent observers, with respect to the staining intensity {negative (−), faintly stained (+) or intensely stained (++)}.

The anti-human PDIA3 antibody is an affinity-purified rabbit polyclonal antibody raised against a 20 amino acids synthetic peptide corresponding to residues 1 to 20, which map to the amino terminus of human PDIA3. This antibody is reported to react specifically with PDIA3 of mouse, rat and human origin and has been used previously for immunohistochemical investigation of PDIA3 localization in normal and neoplastic human tissues. Serum PDIA3 level was quantified using an enzyme-linked immunosorbent assay (ELISA).

Evaluation of mRNA expression of PDIA3

The PCR primers were designed from annotated expressed sequence tags (EST) sequences of PDIA3, obtained from the Salmon Genome Project (SGP) database (www.salmongenome.no/cgi-bin/sgp.cgi). RT-PCR was performed using 0.5 µg of total RNA and the one-step RT-PCR kit from Invitrogen Ltd, Paisley, UK. The 5'-end of PDIA3 cDNA was obtained by using the 5' GeneRacer kit (Invitrogen Ltd, Paisley, UK) with primers described in the kit.

The PDIA3 (418 bp), 5'-CTCCTCGCCTCCGCCTCAGA-3' (forward) and 5'-AGCCCACCACCGAGGCATCT-3' (backward). β-actin (302bp), 5'-GTGGACATCCGCAAAGAC-3' (forward) and 5'-AAAGGGTGTAACGCAATCAA-3' (backward). The PCR program was as follows: 1 min at 95°C, 1 min at 56°C, and 1 min at 72°C for 30 cycles. The PCR products were then subcloned into the TOPO-TA cloning vector (Invitrogen Ltd, Paisley, UK). Sequencing was performed in both directions by the dideoxy chain termination method, using sequencing mixes (Amersham Pharmacia Biotech). The comparison of cDNA sequences was analyzed with the Vector NTI software (Invitrogen Ltd, Paisley, UK).

Western blot analysis

Western blotting was performed according to standard procedures. Protein samples were subjected to 10% SDS–PAGE, transferred to the nitrocellulose membrane, and blocked with TBS-T (20 mM Tris (pH 7.6), 150 mM NaCl and 0.1% Tween-20) containing 3% BSA. The membrane was incubated with anti-human FcεRI antibody (1:500 dilution) and anti-mouse immunoglobulin HRP antibody (1:2000 dilution). The immunoreactive proteins were visualized using the enhanced chemiluminescent ECL assay kit (Amersham Pharmacia Biosciences, NJ, USA), according to the manufacturer's instructions. Western blot bands were visualized using LAS3000® Luminescent image analyzer (Fujifilm Life Science, Tokyo, Japan).

Statistics

All data are presented as means ± SE. The results were calculated statistically using 1-way analysis of variance (ANOVA) and the Duncan multiple range test. Differences were considered to be significant at $P < 0.05$. The calculations were made using the STATISTICA software package version 6.0 (StatSoft Corp, Krakow, Poland).

RESULTS

Levels of serum creatinine after renal transplantation

The levels of serum creatinine in the experiment group and control group were shown in Table 1. Before operation, there were no statistical difference ($p>0.05$) in serum creatinine levels. Seven days after operation, levels of serum creatinine in the experiment group were significantly ($p<0.05$) higher than that of the control.

Histopathological examination of transplanted kidney

Obvious cell immune injury was observed in the experiment group (Figure 1). Severe inflammatory cell infiltration was observed around the renal tubular and capillaries among animals in the experiment group. Renal tubular necrosis, tubular dilatation, and arteriolar wall fibrosis were also detected. Cell infiltration interstitial dilatation and fibrosis was less frequent in the control group than in the experiment group (Figure 2).

Two-dimensional difference gel electrophoresis analysis of transplanted kidney

The 2D pattern differences of the renal tissues between

Table 1. Comparison of serum creatinine level between the experimental and control groups ($\bar{x} \pm s$, μmol/L).

Group	n	Before operation	After operation
Experiment group	8	47.12±4.36*	543.4±53.88**
Control group	8	48.79±4.21	41.87±4.55

* P>0.05, vs .control group, ** P<0.01, vs. control group.

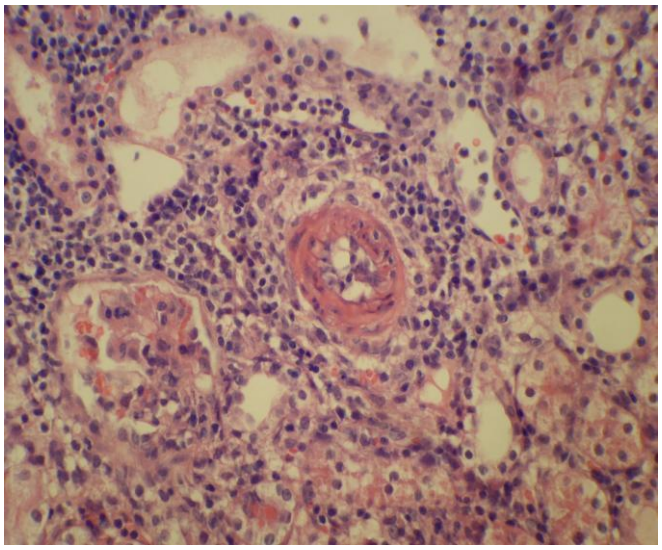

Figure 1. Histopathology alteration by HE staining at day 7 posttransplant in the experimental group (HE×400).

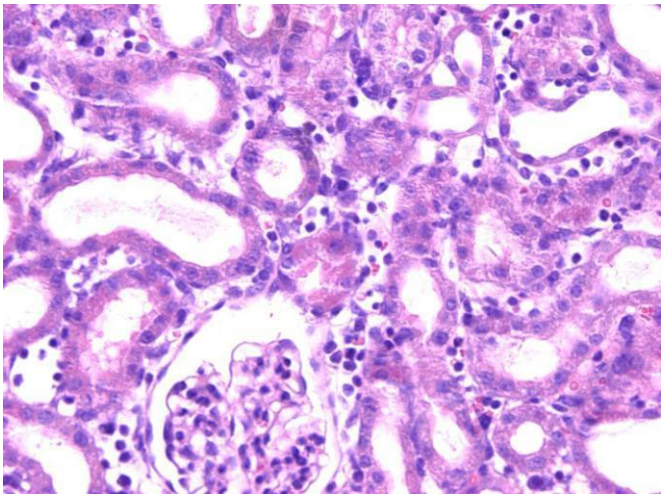

Figure 2. Histopathology alteration by HE staining at day 7 posttransplant in the control group (HE×400).

the experiment and control group were shown in Figures 3 and 4. In both groups, the renal tissue protein samples were separated by 2D-PAGE. The analysis on the high-

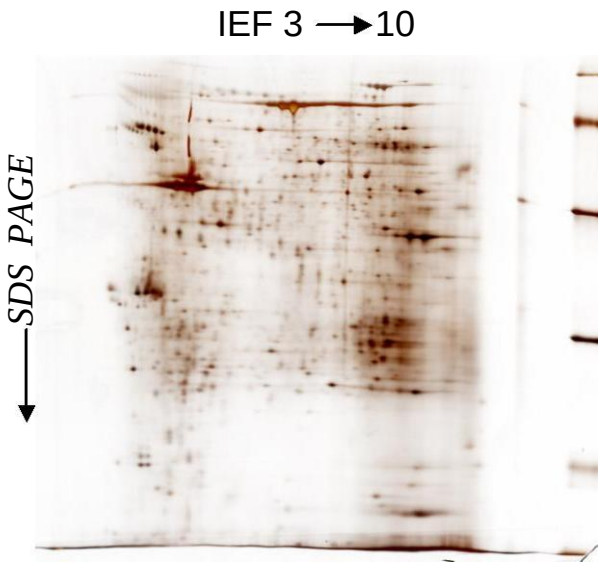

Figure 3. Protein 2-D gel electrophoresis analysis of transplanted kidney in experiment group.

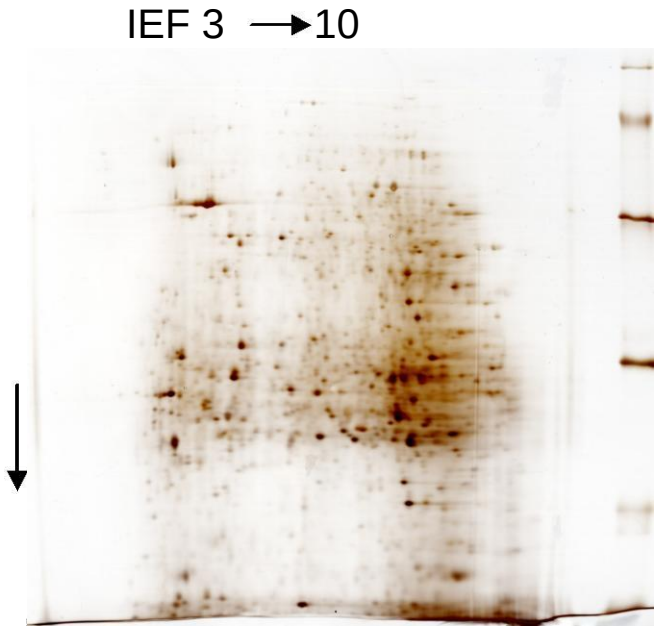

Figure 4. Protein 2-D gel electrophoresis analysis of transplanted kidney in control group.

resolution areas suggested that under the same condition, 2DE patterns were obtained with high-resolution and satisfactory-repetition after 2DE was performed 3 times in one of the samples. PDQuest software 8.1.0 analysis indicated that molecular weight of protein spots was from 10 to 100 kD. There were 554 ± 34 protein spots and 542 ± 21 protein spots in experiment and control groups, respectively. Quantitative difference analysis showed that expression levels of 37 protein

Table 2. Differentially expressed protein spots of transplanted kidney in experiment group.

No	Proteins	NCBI accession numbers	Molecular weight (Da)	Isoelectric point	Sequence coverage (%)	Differentially expression level	t -test	Score
1	Tropomyosin beta chain	500450	32931	4.66	23	5.09	0.00021	63
2	Protein disulfide-isomerase A3	29468	57044	5.88	36	3.53	0.00051	120
3	ADP-ribosylation factor 5	79117	20631	6.30	48	4.54	0.00034	62
4	Alpha-1-antiproteinase	24648	46278	5.70	25	3.41	0.00059	77
5	cyclin-dependent kinase 6	114483	36939	6.00	29	-4.74	0.00029	53
6	NIMA-related kinase2	819641	35094	6.30	31	-5.29	0.00018	70

Table 3. Comparison of serum PDIA3 expression level between the experimental group and control group ($\bar{x} \pm S$, pg/ml).

Group	n	Before operation	After operation
Experiment group	8	89.11±13.00*	361.07±30.90 **
Control group	8	87.64±15.32	281.58±24.02

* P>0.05, vs. Control group, ** P<0.01, vs. experiment group

Table 4. Comparison of PDIA3 mRNA expression level between the experimental and control groups ($\bar{x} \pm S$).

Group	n	PDIA3 mRNA
Experiment group	3	0.821±0.046
Control group	3	0.187±0.154

P<0.01, vs. control group

Table 5. Comparison of PDIA3 protein expression level between the experimental and control groups ($\bar{x} \pm S$).

Group	n	PDIA3 protein
Experiment group	3	0.812±0.047
Control group	3	0.237±0.134

P<0.01, vs. control

spots significantly changed in the experiment group, when the difference of value of the total optical density reached 3 time (Figures 3 and 4). Among them, expression levels of 24 protein spots were up-regulated, while expression levels of 13 protein spots were down-regulated. The aforestated results showed that the 2DE technique used in this study for renal tissue analysis demonstrated desirable repetition (90.1 and 89.2%).

MS identification of differentially expressed proteins

An analysis by MALDI-TOF-TOF-MS was performed after the enzymolysis of the protein spots in the gels. Among 37 protein spots, 29 obtained satisfactory peptide mass fingerprinting (Figure 5). Six differentially expressed protein spots were identified by MS/MS between groups (Table 2).

Serum PDIA3 level

PDIA3 positive staining was yellow particles and is expressed mainly in cytoplasm. Its positive or strong positive expression in transplanted kidney was detected in experiment group (Figure 6). But its expression in transplanted kidney showed weak positive in control group (Figure 7). There was no significant statistical difference (p>0.05) in serum PDIA3 level, between groups before operation. At day 7 after operation, serum PDIA3 level in experiment group was significantly (p<0.05) higher than that in control group (Table 3).

Expression of PDIA3 mRNA in transplanted kidney

Expression levels of PDIA3 mRNA in transplanted kidney of experiment and control groups were shown in Table 4 and Figure 8. PDIA3 mRNA expression level in experiment group was significantly (p<0.05) higher than that in the control group.

Expression level of PDIA3 protein in transplanted kidney

Expression levels of PDIA3 protein in transplanted kidney of experiment and control groups were showed in Table 5 and Figure 9. PDIA3 protein expression level in experiment group was significantly (p<0.05) higher than that in the control group.

DISCUSSION

Rejection is the major cause of graft failure, and if the injury to the tubules and glomeruli is severe, the kidney

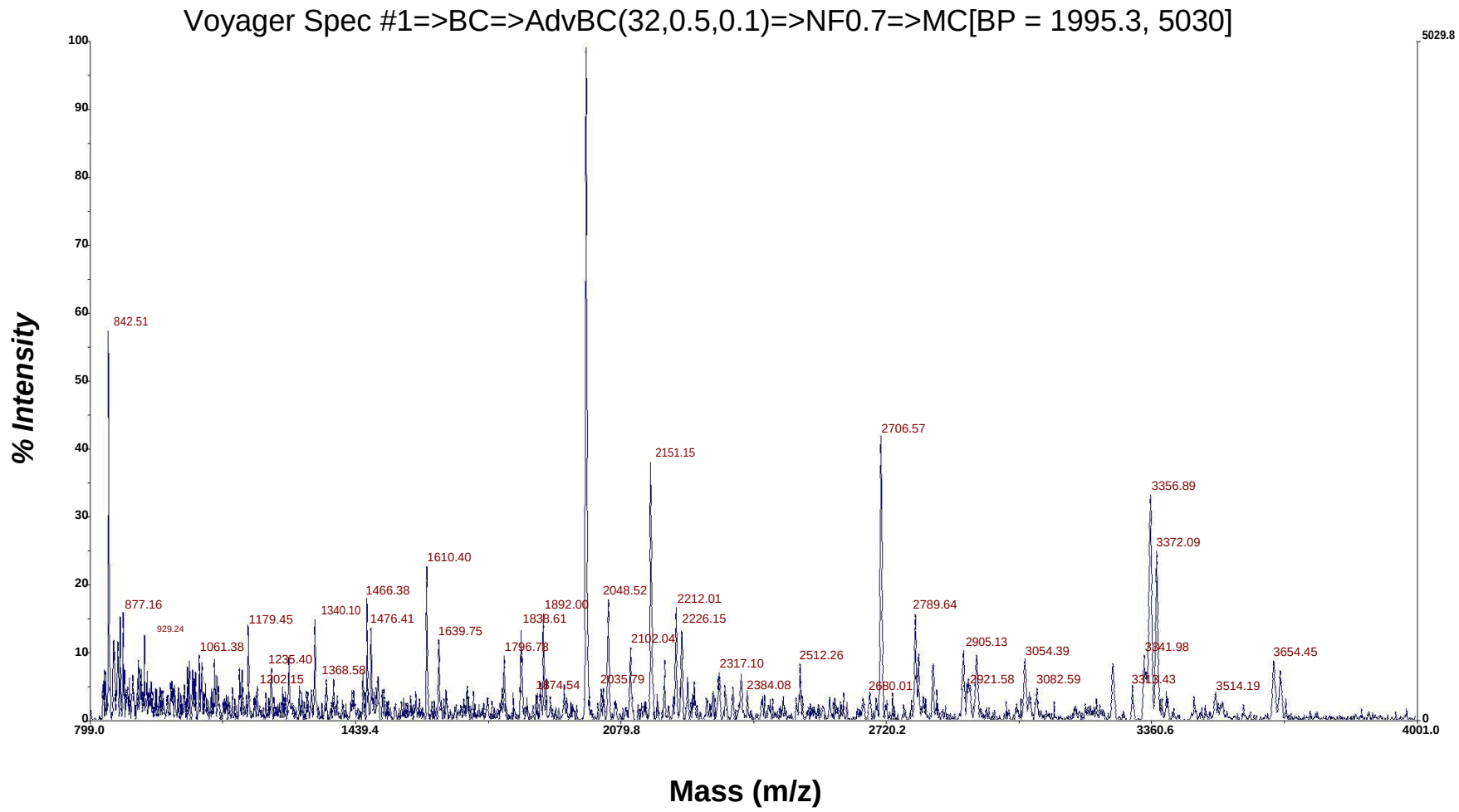

Figure 5. Peptide mass fingerprinting of PDIA3.

may not recover. It is therefore important to diagnose acute rejection as soon as possible to institute prompt antirejection therapy. Generally, the success with which transplant (Terasaki et al., 1996; Chan and Kam, 1997). At present, the mechanisms underlying renal allograft rejection remains unclear. In this study, we utilize proteomics technology to analyse differentially expressed proteins in acute rejection response of rat allogeneic kidney transplantation and to establish 2D electrophoretic spectra. We expect to explore molecular mechanisms of acute rejection after renal transplantation and find out some new biomarkers related to transplant rejection and kidney failure.

In the present study, we investigated differentially expressed proteins in allograft rejection group and isograft control group using two-

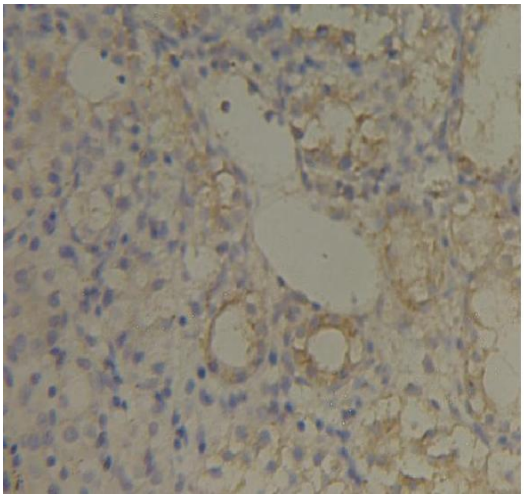

Figure 6. PDIA3 expression in renal allografts of experimental group (×400).

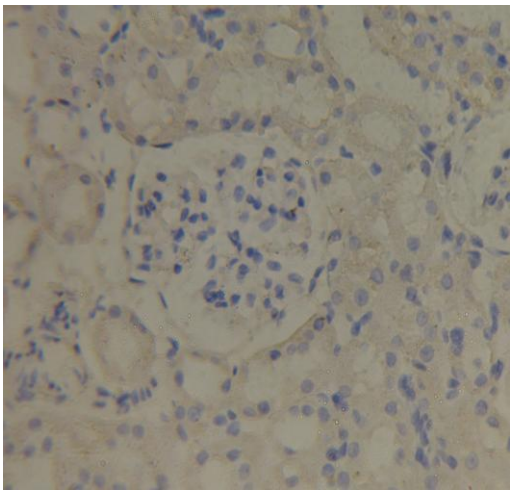

Figure 7. PDIA3 expression in renal allografts of control group (×400).

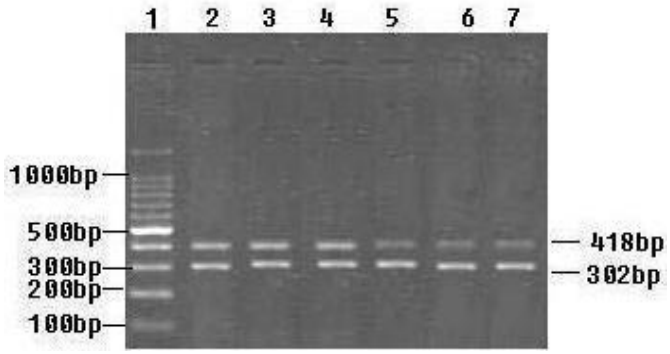

Figure 8. PDIA3 mRNA expression in the experimental and control groups. 1. 100bp DNA maker, 2, 3 and 4 (experiment groups), 5, 6 and 7 (control groups).

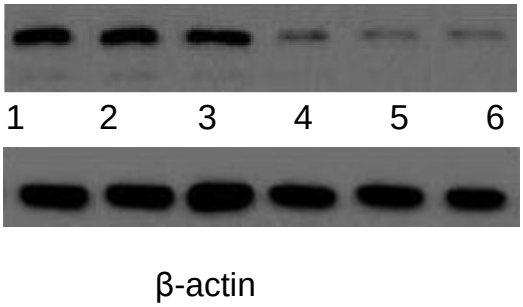

Figure 9. Western-blotting results of PDIA3 in the experimental and control groups. 1, 2 and 3 (experiment groups), 4, 5 and 6 (control groups), β-actin (internal reference marker).

dimensional electro-phoresis. Marked change in expression level of 37 protein spots was observed in allograft rejection group. Among them, expression levels of 24 protein spots were up-regulated, while expression levels of 13 protein spots were down-regulated. Among 37 protein spots, 29 obtained satisfactory peptide mass fingerprinting. Protein identification was done using the Mascot software. Six proteins (Protein disulfide-isomerase A3, Tropomyosin beta chain, ADP-ribosylation factor 5, Alpha-1-antiproteinase, cyclin-dependent kinase 6 and NIMA-related kinase2) were identified. Protein disulfide-isomerase A3 was closely associated with immunity injury and stress response. Therefore, we investigated its levels in serum and transplanted kidney, PDIA3 mRNA and protein expression level.

Tropomyosin beta chain

The roles of tropomyosins in stabilising the thin (actin) filament of the sarcomere (Cooper, 2002) and in regulating muscle contraction (Gordon et al., 2000) have been well defined in skeletal muscle. The tropomyosins exist as coiled-coil homo- or heterodimers forming head-to-tail polymers, running along the length of the actin molecule (Li et al., 2010; Matsumura et al., 1983; Holmes et al., 1990; Lin et al., 1997). They are encoded by four different genes; αTm, that is, TPM1 (OMIM 191010), βTm, that is, TPM2 (OMIM 190990), γTm, that is, TPM3 (OMIM 191030), and δTm, that is, TPM4 (OMIM 600317) (Martin et al., 2010), generating more than 40 different tropomyosin isoforms due to the use of different promoters or variable intragenic splicing (Martin et al., 2010; Dufour et al., 1998; Cooley and Bergstrom, 2001). Our work showed that TMβ level increased in acute rejection response of renal transplantation. This might be associated with its modifying cell activities and skeleton structure, and inducing cell apoptosis.

ADP-ribosylation factor 5

ADP-ribosylation factors (ARFs) belong to a subgroup of

the ras superfamily of 20 kDa GTP-binding proteins. Initially identified through *in vitro* studies as cofactors of the cholera toxin-catalyzed ADP-ribosylation of the heterotrimeric G proteins, they have been shown to be involved in membrane trafficking and activation of phospholipase D (Nara et al., 2010; Moss and Vaughan, 1995; Moss and Vaughan, 1998). ARF has another established role in the transport of intracellular vesicles (Rothman, 1994; Itzen and Goody, 2011), and so may have a central regulatory function in the secretory process of exocrine glands, including salivary acinar cells. Our work showed that ARF5 protein level increase in acute rejection response of renal transplantation. This might indicate that cells apoptosis and necrosis increase due to cell immune injury. Recent studies show that reorganization of cytoskeleton might play an important role in cells apoptosis and necrosis.

Alpha-1-antiproteinase

Alpha 1-Antitrypsin or α1-antitrypsin (A1AT) is a protease inhibitor belonging to the serpin superfamily. It is generally known as serum trypsin inhibitor. Alpha 1-antitrypsin is also referred to as alpha-1 proteinase inhibitor (A1PI) because it inhibits a wide variety of proteases (Gettins, 2002). It protects tissues from enzymes of inflammatory cells, especially neutrophil elastase, and has a reference range in blood of 1.5 to 3.5 g/L (in US the reference range is generally expressed as mg/dl or micromoles), but the concentration can rise many fold upon acute inflammation (Kushner and Mackiewicz, 1993). In its absence, neutrophil elastase is free to break down elastin, which contributes to the elasticity of the lungs, resulting in respiratory complications such as emphysema, or COPD (chronic obstructive pulmonary disease) in adults and cirrhosis in adults or children. Our work showed that A1AT protein level increased in acute rejection response of renal transplantation. A possible explanation is that cells are in immune inflammatory status in acute rejection response of renal transplantation. A1AT protein, an acute phase protein, significantly increases and subsequently results in kidney injury.

Cyclin-dependent kinase 6

Cyclin-dependent kinases (CDKs), such as CDK1, CDK2, and CDK4, constitute a class of serine–threonine protein kinases that plays an important role in regulation of the cell cycle (Harper and Adams, 2001). Abnormal CDK control of the cell cycle has been strongly linked to the molecular pathology of cancer. CDKs have thus become attractive therapeutic targets for cancer therapy (Sielecki et al., 2000). The CDKs regulate cell cycle progression through complexes with their corresponding cyclin partners such as cyclin A, B, D, and E. For example, CDK1 associated with cyclin B regulates the cell cycle at the G2 and mitosis (cell division) phases. In this work, CDK6 protein level was decreased in acute rejection response of renal transplantation. This might be related to increased apoptosis and necrosis due to cell immunity injury. Reduced CDK6 level inhibits endogenous regulation of the cell cycle and make cells stagnate at G1 phase of cell cycle. Subsequently, this inhibits cell division and promotes apoptosis.

NIMA-related kinase2

Nek2 (NIMA-related kinase2) is a mammalian kinase structurally related to the protein kinase NIMA of *Aspergillus nidulans* that is required for entry into mitosis. Temperature-sensitive mutations of NIMA reversibly arrest cells in late G2 (Brzywczy et al., 2011), despite the presence of activated $p34^{cdc2}$ kinase activity, indicating that NIMA function, plays an essential role downstream or parallel to $p34^{cdc2}$ for progression through mitosis (Osmani et al., 1991). Although phosphorylation of NIMA by $p34^{cdc2}$/cyclin B is not required for basal level NIMA kinase activity, it appears to be required for mitotic entry (Ye et al., 1995). In this work, Nek2 protein level decrease in acute rejection response of renal transplantation. Reduced Nek2 protein expression might delay cell replication, division and proliferation phase.

Protein disulfide isomerase A3

The protein disulfide isomerase (PDI) is a multifunctional protein that participates in protein folding, assembly, and post-translational modification in the endoplasmic reticulum (ER) (Wilkinson and Gilbert, 2004). PDI catalyzes both the oxidation and isomerization of disulfides of nascent polypeptides. It functions both as an enzyme and as a chaperone. As an enzyme, it increases the rate of disulfide bond formation without altering the folding pathway (Noiva, 1999). As a chaperone, it promotes correct folding of proteins by preventing the misfolding and aggregation of partially folded or misfolded peptides (Noiva, 1999). PDI has been shown to be essential in the cell biosynthesis pathway and to play a role in cell–cell interaction and the regulation of some receptor functions (Frand et al., 2000).

Protein disulfide isomerase associated 3 (PDIA3/ERP57), a member of the PDI family, can catalyze the oxidation, reduction and isomerization of intra- and intermolecular disulfide bonds to ensure the correct folding of secretory proteins prior to their further modification and transport in the endoplasmic reticulum (ER) (Honjo et al., 2010). PDIA3/GRP58 binds to specific DNA sequences, encoding DNA repair proteins, which suggests they play a role in regulating stress-response

genes (Chichiarelli et al., 2007).

In the present study, two-dimensional difference gel electrophoresis analysis showed that expression level of PDIA3 mRNA was up-regulated in rat allograft group. This level is 3.53 times as much as that in isograft group. Western blot and RT-PCR analysis confirm the result. Moreover, the result is also supported by serum PDIA3 content and localization analysis of transplanted kidney. We think that receptor signing transduction pathway change much after acute rejection in renal transplantation. Subsequently, serum PDIA3 level also changed. PDIA3 might be involved in the occurrence and development of acute rejection response in renal transplantation. How does PDIA3 involve in receptor signing transduction pathway? How does it affect the pathophysiological procedure of acute rejection response in renal transplantation? This will be investigated in future study.

REFERENCES

Brzywczy J, Kacprzak MM, Paszewski A (2011). Novel mutations reveal two important regions in Aspergillus nidulans transcriptional activator MetR. Fungal Genet. Biol. 48:104-112.

Chichiarelli S, Ferraro A, Altieri F, Eufemi M, Coppari S, Grillo C, Arcangeli V, Turano C (2007). The stress protein ERp57/GRP58 binds specific DNA sequences in HeLa cells, J. Cell. Physiol. 210:343–351.

Chan L, Kam I (1997). Outcome and complications of renal transplantation. In Diseases of the Kidney, edn 6. Edited by Schrier RW, Gottschalk CW.

Cooley B, Bergstrom G (2001). Multiple combinations of alternatively spliced exons in rat tropomyosin-alpha gene mRNA: evidence for 20 new isoforms in adult tissues and cultured cells. Arch. Biochem. Biophys. 390:71–77.

Cooper (2002). Actin dynamics: tropomyosin provides stability. Curr. Biol. 12:R523–525.

Diamandis EP (2004). Mass spectrometry as a diagnostic and a cancer biomarker discovery tool: Opportunities and potential limitations. Mol. Cell Proteomics 3:367-368.

Dufour C, Weinberger R, Schevzov G, Jeffrey P, Gunning P (1998). Splicing of two internal and four carboxyl-terminal alternative exons in nonmuscle tropomyosin 5 pre-mRNA is independently regulated during development. J. Biol. Chem. 273:18547–18555.

Frand AR, Cuozzo JW, Kaiser CA (2000). Pathways for protein disulphide bond formation, Trends Cell Biol. 10:203–210.

Gettins PG (2002). Serpin structure, mechanism, and function. Chem. Rev. 102:4751–804.

Gordon A, Homsher E, Regnier M (2000). Regulation of contraction in striated muscle. Physiol. Rev. 80:853–924.

Harper JW, Adams PD (2001). Cyclin-Dependent Kinases. Chem. Rev. 101:2511-2526.

Holmes K, Popp D, Gebhard W, Kabsch W (1990). Atomic model of the actin filament. Nature 347:44–49.

Honjo Y, Ito H, Horibe T, Takahashi R, Kawakami K (2010). Protein disulfide isomerase-immunopositive inclusions in patients with Alzheimer disease. Brain Res. 1349:90-96.

Itzen A, Goody RS (2011). GTPases involved in vesicular trafficking: Structures and mechanisms. Semin. Cell Dev. Biol. 22:48-56.

Keeping A, DeAbreu D, DiBernardo M, Collins RA (2011). Gel-based mass spectrometric and computational approaches to the mitochondrial proteome of Neurospora. Fungal Genet. Biol. 48:526-536.

Kushner I, Mackiewicz A (1993). The acute phase response: an overview. CRC Press pp. 3–19.

Li XCE Lehman W, Fischer S (2010). The relationship between curvature, flexibility and persistence length in the tropomyosin coiled-coil. J. Struct. Biol. 170:313-318.

Lin JJC, Warren KS, Wamboldt DD, Wang T, Lin JLC (1997). Tropomyosin isoforms in nonmuscle cells. Int. Rev. Cytol., 170: 1–38.

Martin C, Schevzov G, Gunning P (2010). Alternatively spliced N-terminal exons in tropomyosin isoforms do not act as autonomous targeting signals. J. Struct. Biol. 170:286-293.

Matsumura F, Yamashiro MS, Lin J (1983). Isolation and characterization of tropomyosin-containing microfilaments from cultured cells. J. Biol. Chem. 258:6636–6644.

Moss J, Vaughan M (1995). Structure and function of ARF proteins. Activators of cholera toxin and critical components of intracellular vesicular transport processes. J. Biol. Chem. 270:12327–12330.

Moss J, Vaughan M (1998). Molecules in the ARF orbit. J. Biol. Chem. 273:21431–21434.

Nakao A, Faleo G, Nalesnik MA, Seda NJ, Kohmoto J, Murase N (2009). Low dose carbon monoxide inhibits progressive chronic allograft nephropathy and restores renal allograft function. Am. J. Physiol. Renal Physiol. 297:F19–F26.

Nara A, Aki T, Funakoshi T, Uemura K (2010). Methamphetamine induces macropinocytosis in differentiated SH-SY5Y human neuroblastoma cells. Brain Res. 1352:1-10.

Neto JS, Nakao A, Toyokawa H, Nalesnik MA, Romanosky AJ, Kimizuka K, Kaizu T, Hashimoto N, Azhipa O, Stolz DB, Choi AM, Murase N (2006). Low-dose carbon monoxide inhalation prevents development of chronic allograft nephropathy. Am. J. Physiol. Renal Physiol. 290:F324–F334.

Noiva R (1999). Protein disulfide isomerase: the multifunctional redox chaperone of the endoplasmic reticulum, Semin. Cell Dev. Biol. 10:481–493.

Osmani AH, McGuire SL, Osmani SA (1991). Parallel activation of the NIMA and p34cdc2 cell cycle-regulated protein kinases is required to initiate mitosis in A. nidulans. Cell 67:283-291.

Pan TL, Wang PW, Huang CC, Goto S, Chen CL (2004). Expression, by functional proteomics, of spontaneous tolerance in rat orthotopic liver transplantat. Immunol. 113:57–64.

Rothman JE (1994). Mechanisms of intracellular transport. Nature 372:55–63.

Sielecki TM, Boylan JF, Benfiled PA, Trainor GT (2000). Cyclin-dependent kinase inhibitors: Useful targets in cell cycle regulation. J. Med. Chem. 43:1-18.

Terasaki PI, Cecka JM, Gjertson DW, Takemoto S, Cho YW, Yuge J (1996). Risk rate and long-term kidney transplant survival. Clin. Transpl. p. 443.

United Network for Organ Sharing (1994): The UNOS Statement of Principles and Objectives of Equitable Organ Allocation. UNOS Update 10:20.

Vestal ML, Juhasz P, Martin SA (1995). Delayed extraction matrix-assisted laser desorption time-of-flight mass spectrometry. Rapid Commun. Mass Spectrom. 9:1044-1050.

Wilkinson B, Gilbert HF (2004). Protein disulfide isomerase. Biochim. Biophys. Acta 1699:35–44.

Wong F (2011). Renal Diseases and the Liver. Clin. Liver Dis. 15:39-53.

Ye XS, Xu G, Pu RT, Fincher RR, McGuire SL, Osmani AH, Osmani SA (1995). The NIMA protein kinase is hyperphosphorylated and activated downstream of p34cdc2/cyclinB: coordination of two mitosis promoting kinases. EMBO J. 14:986-994.